2024 IEEE/ASME International Conference on Advanced Intelligent Mechatronics (AIM)
July 15-19, 2024. Boston, MA, USA

Bioinspired Mechanical Design and Tests of a Humanoid Robot for Highly Dynamic Jumping

Gao Huang[1], Xuefei Zhao[2], Xuechao Chen[3], Zhangguo Yu[4],
Libo Meng[5], Mingfeng Wang[6], Marco Ceccarelli[7], Qiang Huang[8]

Abstract—**Highly dynamic motions, such as jumping, are crucial for biped robots to efficiently traverse challenging terrains and unstructured environments. This paper introduces an optimal design for an electrically actuated humanoid robot, specifically crafted to meet the demands of high dynamic jumping motions, with a focus on enhancing impact resisting, ruggedness, and power. Given the profound impact of the robot's actuation and transmission on diverse design specifications (e.g., speed, torque, overall mass, and compactness), special emphasis is placed on the design of joint actuators and the configuration of joint transmissions. The key characteristics achieved include low leg inertia, excellent joint back-drivability, and explosive power output ability, drawing inspiration from the characteristics of human jumping motion. Simulations and experiments of jumping motions validate the feasibility of the new design solutions. Recorded data indicates that the robot can execute explosive jumping motions, and the proposed leg structure can withstand significant impact forces, reaching up to 4.6 times the body weight during stable landing phases. Thanks to the new design of the leg actuator and linkage transmissions, the designed robot can achieve a vertical jump height of 0.5 m and a long jump of 1.0 m without the need for an energy storage system. Notably, through simulation comparisons, our up-shifting inertia design has the potential to reduce joint torque requirements by up to 32.2% during jumping motions.**

Index Terms—**Humanoid robot, dynamic jumping, bioinspired actuator design, transmission design, optimization.**

I. INTRODUCTION

HUMANOID robots have the potential to assist or replace humans in performing several tasks within human living environments, making them highly sought after in areas such as public safety, rescue operations, relief efforts, aging social services, and applications involving dangerous environmental operations and family services [1], [2].The recent announcement about Tesla's development of humanoid robots has ignited a wave of research in the field of humanoid robotics. Jumping motions enable humanoid robots to overcome obstacles that are 3-4 times higher than those navigable through walking. However, the challenge lies in the high dynamic jumping requirements for the robot's actuation and control [3].

Significant advancements have been achieved in the construction of systems and dynamic control of jumping motions [4]. Boston Dynamics consistently introduces new skills each year showcasing the motion capabilities of robots equipped with hydraulic actuators [5]. The Atlas robot can perform intricate dances and backflips. Although Atlas can achieve a jump height of 0.6m, details of the system design and control methods are not publicly disclosed. In the realm of electrically actuated robots, ASIMO can continuously hop but with a lower height. The JAXON3-P robot from the University of Tokyo has realized jumping motions with a 0.3m center of gravity height using force control methods [6]. While Cassie has achieved a jumping height of 0.5m, the Digit is limited to continuous hopping motions [7]. In summary, the current jumping ability of man-sized electrically-driven humanoid robots is limited to around 0.3 m, restricting their mobility and adaptability to complex environments.

The design of actuators constitutes the core of achieving highly dynamic jumping motions in legged robots. Different types of actuators have been introduced to enhance the jumping capabilities of biped robots. Hydraulic actuators, resembling human muscles propulsion mechanism, are effective in withstanding impacts, making them suitable for high dynamic motion robot designs [8]. Another commonly used actuator is the electric-driven actuator, which can be categorized into two groups: those with or without elastic components. The former, known as series elastic actuators (SEAs), and the latter can be further categorized into high and low reduction ratios, the latter referred to as pseudo direct drive (PDD). SEAs are considered promising for the actuation of bio-inspired robots. ETH Zurich proposed a coupling-based SEA for hopping or running locomotion, featuring the ability to engage and disengage the connection between an actuation element and a mechanical spring [9]. The Italian Institute of Technology (IIT) introduced both series- and parallel-elastic series-parallel actuation, significantly improving energy efficiency [10]. SEAs provide a certain level of elasticity to absorb impact and enhance energy efficiency. However, their force control bandwidth is relatively low, potentially falling short of the rapid

*This work was supported by the National Natural Science Foundation of China under Grant 62103053. (Corresponding author: Gao Huang)

[1]G. Huang, [2]X. Zhao are with the Faculty of Information Technology, Beijing University of Technology, Beijing 100124, China (e-mail: huanggao@bjut.edu.cn; zhaoxuefei@bjut.edu.cn).

[3]X. Chen, [4]Z. Yu, and [8]Q. Huang are with the Intelligent Robotics Institute, School of Mechatronical Engineering, Beijing Institute of Technology, Beijing 100081, China, and also with the International Joint Research Laboratory of Biomimetic Robots and Systems, Ministry of Education, Beijing 100081, China (e-mail: chenxuechao@bit.edu.cn; menglibo@bit.edu.cn; yuzg@bit.edu.cn; qhuang@bit.edu.cn).

[5]L. Meng is with the Qiyuan Laboratory, Haidian District, Beijing 100095, China (e-mail: menglibo@outlook.com).

[6]M. Wang is with the Department of Mechanical and Aerospace Engineering, Brunel University London, UB8 3PH London, U.K. (e-mail: mingfeng.wang@brunel.ac.UK).

[7]M. Ceccarelli is with Department of Industrial Engineering, University of Rome Tor Vergata Via del Politecnico 1, Roma 00133, Italy (e-mail: marco.ceccarelli@uniroma2.it).

response requirements for high dynamic motions. The low-frequency dynamic response capability has been eliminated from the drive scheme of high gear ratio harmonic reducers and the SEA scheme commonly used in humanoid robots. A notable example of PDD is the proprioceptive actuator proposed by MIT, comprising a high torque density motor (T-Motor) and a low reduction ratio planetary gearbox (7.67:1). This configuration allows for relatively high torque density, excellent back-drivability, and a high force control bandwidth. Using this actuator, the MIT Cheetah 3 quadruped robot can repeatedly jump onto and down from a desk with a height of 0.76 m [11]. However, due to the lower reduction ratio and limited output capacity of motors, the torques generated by PDD actuators may not be sufficient for the highly dynamic motions of human-sized biped robots.

Another crucial aspect for enhancing the highly dynamic motion capabilities of legged robots is the design of a specific transmission mechanism [12]. The biped robot system represents a complex electromechanical integrated dynamic system with multiple rigid bodies. Placing the drive at the joints can generate constant torque independent of joint angle, simplifying the kinematics solution, but it results in substantial leg inertia, failing to meet the dynamic requirements of high dynamic motions. Linkage mechanisms, such as the four-bar mechanism, crank-rocker mechanism, and slider-crank mechanism, offer variable torque, allowing for the optimization of torque output to meet the demands of high dynamic motions, as observed in the reported experience [13].

The primary reason for the insufficient jumping ability of humanoid robots can be attributed to the fact that electric-driven humanoid robots are typically equipped with high gear ratio and high-rigidity actuators. Constrained by volume and weight limitations, these joints lack explosive capability and cannot provide sufficient energy within the limited jumping time, consequently restricting the robot's jumping height and distance. Simultaneously, inadequacies may arise from the transmission mechanism when it is not specifically designed in accordance with the characteristics of jumping motion. Furthermore, as the jumping height increases, the instantaneous impact during takeoff and landing rises sharply [14], posing a significant challenge to the overall robot design.

This paper specifically addresses the deficiencies mentioned above by focusing on the characteristics of jumping motion. The key contributions of this paper can be outlined as follows:

1) Proposing a bio-inspired design method for a biped robot with enhanced jumping ability. A detailed method is introduced for the design and optimization of ball screw-based linear actuators and plenary actuators, emphasizing their properties and linkage parameters.
2) Introducing the design of an up-shift inertia leg and quantitatively analyzing its impact on joint torque requirements.
3) Realizing good back-drivability, impact assist ability, and joint power output capability through the proposed system design, validated quantitatively through experiments.

The rest of this article is organized as follows. In Section II, we analyze the jumping motion of the human and propose a mathematical model for robot jumping motion. A design scheme is then proposed. In Section III, the proposed scheme is implemented on the robot's mechanical design, and the robot's designed structures are optimized with Finite Element Analysis (FEA). In Section IV, Simulation and experiments are discussed to verify the effectiveness of the proposed method. Finally, Section V concludes this article.

II. Human's Jumping and Robot Design Requirements

After millions of years of evolution, humans have developed strong jumping abilities. Therefore, the design of robots can draw inspiration from the imitation of the human jumping mechanism. Consequently, this paper first examines the actuation mechanism and motion characteristics of human jumping.

A. Human's Jumping

In order to study the posture control characteristics and analyze the laws of kinematics and dynamics in the process of human jumping, a motion capture system is designed. It mainly includes MVN Link Lycra suit, control computer, a high-speed camera and six-dimensional force sensor platform.

In order to reduce the accidental error of the experiment and obtain more universal rules from the collected motion data, 4 volunteers are randomly selected with similar height, weight, and age, and each volunteer conducted six repeated jumping experiments. The jumping motion data of these 4 volunteers are recorded in real time by the motion capture. This experiment mainly studies human high jump and focuses on the coordinated motion between the leg joints (hip joint, knee joint and ankle joint) of the human body.

The snapshot of human jumping motion captured by high-speed camera during the process is shown in Fig. 3. According to Fig. 3, human jumping motion can be divided to four distinct phases: the squatting phase, pushing phase, flying phase and landing phase. In the context of human biomechanics, during the squatting phase, the process of executing a vertical jump commences with the contraction of the body to accumulate energy for takeoff. As the body reaches its nadir of contraction, muscular energy is subsequently released, propelling both feet off the ground. Upon entering the flight phase, deceleration of the limbs is orchestrated, maintaining a specific posture until the descent, at which point the feet contact the ground once more. Through the orchestration of postural adjustments, the human body attenuates the impact forces, culminating in a smooth and controlled landing.

Fig. 1 illustrates a set of representative data calculated for leg joints, including joint angular velocities, torques, powers in a vertical jump of approximability 0.5 m.

The results of joint velocities, torques, and power calculations can serve as important references for analyzing joint requirements and optimizing parameters in robotics design. From Fig. 1, it can be observed that the duration of a single jumping motion is very short, with takeoff and landing times

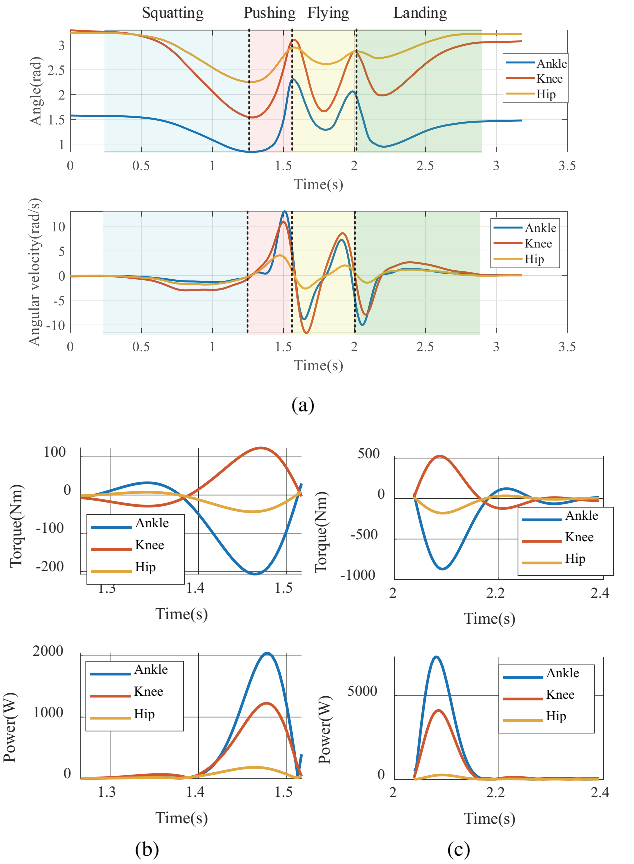

Fig. 1. Lower limb joints movement data during jump. (a) Joint angles and angular velocities. (b) Joint torques and power variation at pushing. (c) Joint torques and power variation at landing.

both around 0.2 s to 0.25 s. The focus here is primarily on the leg motions of jumping, involving the ankle joint, knee joint, and hip joint in the sagittal plane. The knee joint serves as the main force-generating joint, while the hip joint and ankle joint also play roles in adjusting the center of mass position. The following patterns can be discerned from Fig. 1:

(1) After the human body squats, starting from the minimum joint angles to the early stage of pushing off the ground, the joint torques quickly reach their maximum values. Around 1.46s, the joint angles for the ankle, knee, and hip joints are 1.2296, 2.2342, and 2.6624 (rad) respectively. At this point, the joint torque reaches its maximum values of -207.0198, 123.6339, -43.3543 (Nm), while the joint velocities are 7.0159, 8.3128, 3.9617 (rad/s), respectively, still increasing.

(2) As the joints exert force, in the later stage of pushing off the ground, the joint angles continue to increase, their velocities gradually increase, and the torques continuously decrease. Around 1.51s, the joint angles for the ankle, knee, and hip joints are 1.8874, 2.7615, and 2.8533 (rad), respectively. At this time, the joint motion velocities reach 13.0327, 10.7607, 4.098 (rad/s), while the driving torques gradually decrease to near zero. This is because in the later stage of pushing, the body is leaving the ground, and no longer requires support.

(3) In the initial stage of landing, the joint angles are relatively large. At this moment, the lower limb joints suddenly experience an impact force, requiring rapid joint response to for leg retraction, concurrently with postural adjustments.

(4) In the late stage of landing, the joint angles are diminished, and the motion speed is reduced, but a significant force is imperative to counteract the impact.

Summarizing the entire jumping phase of the human body, the following joint design principles can be derived: when the angles of lower limb joints are small, there is a higher demand for joint torque and a slightly lower demand for velocity; when the angles of lower limb joints are large, there is a higher demand for joint velocity and a lower demand for torque.

It is noteworthy that volunteers tend to incline the ankle joint forward while maintaining a relatively upright posture during jumping. This leads to increased torque on the ankle joint and reduced torque on the hip joint (Fig. 1(c)). From the perspective of designing and controlling robots, optimizing the robot's performance can be achieved by slightly decreasing the ankle joint angle and slightly increasing the hip joint angle to evenly distribute pressure on both joints.

B. Robot's Design Requirements for Dynamic Jumping

The dynamic jumping ability inherent in humans can be perceived as nature's mechanism for addressing various trade-offs: balancing the capacity to handle significant ground reaction forces while minimizing leg inertia, managing the trade-off between generating high torque during takeoff and achieving high-speed upon leaving the ground, and striking a balance between generating substantial joint toque and maintaining lightweight. According to above analysis, the design requirements for dynamic jumping can be inferred as follows:

(1) High-frequency dynamic response capability. In order to attain a high dynamic jumping capability, it is imperative for joints to exhibit two key characteristics: a high output speed and a high frequency response in terms of force and position. Achieving this necessitates the utilization of a lower gear ratio, typically falling within 70, coupled with high rigidity. Consequently, a high gear ratio and flexible elements scheme commonly employed in humanoid robots should be eschewed.

(2) Keep the leg inertia low. Fast leg swing during jumping motion also a low moment of inertia of the leg about the hip. Design strategies to keep this low are as follows:

1) Make the weight below hip as light as possible, the design strategy is move motors and transmission components high up into the thigh, which is up-shift leg inertia.

2) Minimize reflected inertia of motor rotors. To improve torque output density of the joint and fulfil low-speed and high-torque working conditions, it is necessary to connect a reducer in series to increase the speed at the motor end and reduce the negative impact of cogging effect.

(3) **Good back-drivability.** The process of taking off and landing is fundamentally symmetrical. During pushing, the robot must achieve a substantial liftoff velocity within an extremely short time (0.2s-0.25s). In contrast, during landing, neglecting factors like air resistance, the robot's theoretical velocity upon contact with the ground is equivalent to liftoff.

TABLE I
JOINT CONFIGURATION OF THE BIO-INSPIRED HUMANOID ROBOT

Joints (Sagittal plane)	Motors	Reducers	Gear ratios	Peak torques/ Speeds		Weights (kg)[a]	Range of joint angle [d]
				Requirements	Designed		
Hip	85x26	Custom-made planetary gear	24.965	139.3Nm/ 10.75 rad /s	206.7 Nm/ 24 rad /s	1.89	-0.82∼1.75
Knee	85x26	Ball screw	31.5:1[a]	260Nm/11.4 rad /s	5.8 kN, 289.8 Nm [c]/ 0.79m/s, 15.7 rad/s [c]	1.81	-2.44∼0
Ankle	70x18	Ball screw	63:1[b]	135.58 Nm/ 12.93 rad/s	4.5 kN, 225 Nm[c]/ 0.5 m/s, 10 rad/s [c]	1.20	-1.05∼1.05[b]

[a] Estimated weight
[b] Maximum value, variable
[c] For a 50 mm crank arm perpendicular to the actuator
[d] The vertical plane is defined as 0, with forward motion considered positive and backward motion considered negative.

To achieve smooth cushioning during landing, the robot's joints need to rapidly rotate in the opposite direction during liftoff, necessitating good back-drivability at each joint.

Therefore, to simultaneously meet torque and velocity requirements while keeping joint power constant, it is imperative to utilize gear reduction ratios that are relatively low and high-torque motors. Additionally, minimizing internal joint interactions and joint transmission forces is crucial.

(4) Capabilities of power generation and output. The execution of jumping motions requires the rapid provision of substantial energy to a robot within a short duration. Consequently, several crucial design considerations must be addressed. Firstly, there is a need to enhance the energy storage and discharge capacity of the battery, ensuring a continuous output of power supply. This necessitates a battery system with suitable input voltage and output current capabilities. In addition, it is essential to provide each joint with the maximum attainable range of motion, enabling prolonged energy delivery. Furthermore, it becomes imperative to match distinct joint gear ratios within specified joint power constraints to accommodate different demands in different jumping phases.

III. MECHANICAL DESIGN

To meet the aforementioned jumping requirements, this paper proposes a leg design solution based on biomimicry, the designed configurations for each joint as shown in Table I. The hip joint utilizes a configuration of torque motor combined with a customized planetary gearbox, capable of outputting the required torque and speed. The planetary gearbox, with a relatively small reduction ratio, exhibits good reverse driving performance and strong impact resistance. Both the knee and ankle joints employ torque motors with ball-screw transmissions, utilizing a linkage transmission method to mimic the muscle-driven structure of human legs.

The mechanical design scheme, as illustrated in Fig. 2, is proposed in this paper to meet the requirements of rapid and impact-resistant jumping motions, aiming to enhance the high dynamic jumping capability of the robot.

In terms of transmission mechanism design, both planetary gear reducers and ball screws inherently possess good shock resistance. In this design, the planetary gear reducer adopts a custom-made NGW two-stage configuration, featuring a unique drum-shaped tooth profile and integrated planetary frame. Additionally, precision hard tooth surface machining technology is employed during the manufacturing process, significantly improving the reducer's load density and structural compactness, thereby effectively enhancing its shock resistance. At the output end, high-strength cross-roller bearings are selected to enhance joint output stiffness and stability. The other end of the joint utilizes deep groove ball bearings for auxiliary support, with the design ensuring that this bearing only bears radial forces and not axial forces.

In ball screw transmissions, the primary consideration lies in the robust thrust-bearing capacity. After the ball screw transmits powerful impact forces to the nut, a steel retaining ring and double-row angular contact ball bearings are used to resist large impact forces, as illustrated in Fig. 2(1). At the connection between the push rod and the thigh plate, the dual-bearing support structure is designed to ensure precision while effectively resisting impact. Since the jumping impact force concentrates on the ankle, a steel shaft combined with needle roller bearings is used for connection in that region, as shown in Fig. 2(4).

Simultaneously, while ensuring strength, it is necessary to minimize transmission friction. Hence, we opt for motors with a relatively small drag torque, ball screw components with a small preload force, and enhance lubrication between bearings and gear teeth by removing dust covers from the bearings.

In terms of mechanism connection design, to withstand significant impact forces and meet high co-axiality requirements, the paper strives to reduce the number of parts through integrated design where feasible, such as the hip joint U-shaped bracket, thigh and calf plates, and the planetary gear reducer's planetary frame. Additionally, at locations where the output shaft bears torque or force, the transmission characteristics are fully considered. The torque is mainly borne between the planetary frame and the output flange, thus adopting a pin connection (Fig. 2(2)). The ball screw nut and end mainly bear tension and compression forces, hence utilizing a threaded connection (Fig. 2(1)), effectively ensuring connection strength and reliability. In summary, the overarching objective is to design a system characterized by high energy efficiency and

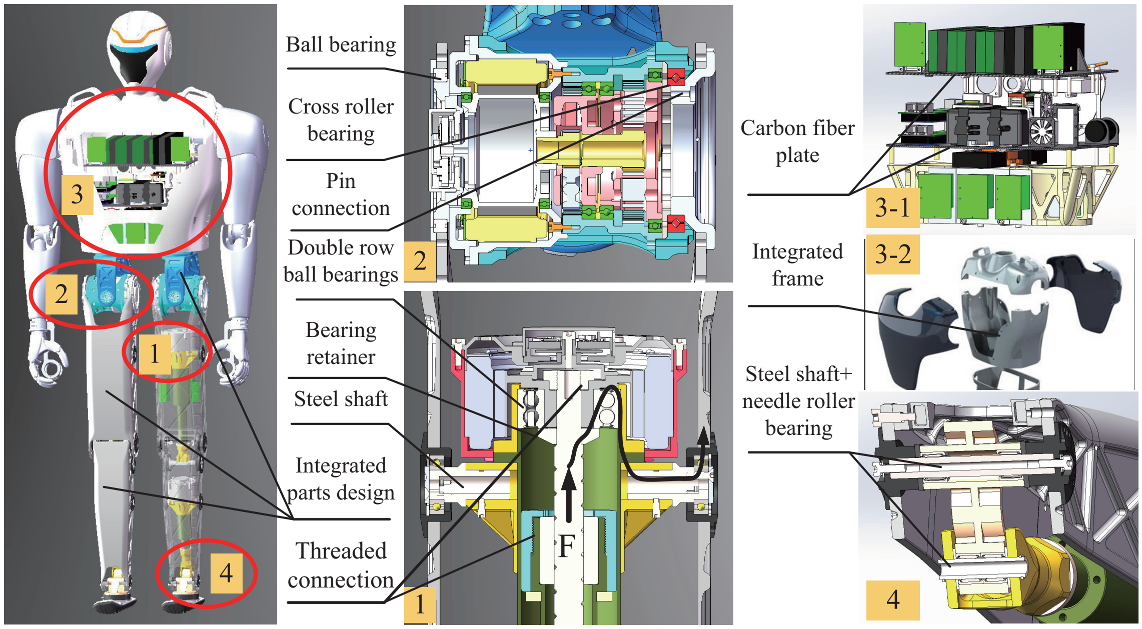

Fig. 2. Mechanical design and detailed solution for impact resisting during jumping.

strong shock resistance.

IV. Robot Jumping Experiments

The prototype has been constructed in accordance with the proposed design, and jumping experiments have been conducted. In the experiment, the robot executed a 0.5m high jump and 1.1m long jump, as depicted in Fig. 3, with the corresponding motion data, the angles, the angular velocities, the torques and the powers of robot leg joint showcased during the robot's jumping sequence in Fig. 4.

As the high jump is similar to the long jump in its motion characteristics, this paper analyzes the motion using the high jump. It is evident that, during the initial phase of pushing off the ground, the robot's leg joints rapidly supplied significant torque. At approximately 0.38s, the ankle, knee, and hip joint angles were measured at 0.8886, 1.4578, and 1.5856 radians, respectively. During this moment, the torque values for the lower limb joints were -79.4946, 132.8379, and -98.7145 Nm, while the joint velocities remained relatively small at 1.6818, 4.3192, and 3.3325 rad/s. In the subsequent phase of pushing off the ground, the robot's leg joints primarily contributed to high velocities. Around 0.46s, the joint angles measured 1.1371, 2.0916, and 2.1188 radians, with corresponding velocities of 3.9437, 9.9888, and 8.6007 rad/s, while the joint torques were comparatively smaller.

Similar patterns are observed during the landing phase. Immediately after landing, when the leg is extended, the robot's joint velocity response is rapid and quickly reaches its maximum. As time progresses, the velocity of joints decreases, while the joint torques continually increase to support the robot and resist the impact force generated during landing.

In the actual robot jumping experiment, the data from the force sensor at the ankle is illustrated in Fig. 5. The robot completes the collision with the ground in less than 0.02 seconds. According to the Theorem of Momentum, $mv = Ft$, the average impact force during the robot's landing should be greater than 7200N, which is at least 15 times the body gravity. Such a significant impact poses substantial challenges to the joint output capacity and stable control of the robot.

The linkage transmission mechanism design allows the joints to respond rapidly within a very short time frame of 0.02 s when dealing with substantial ground impact, thereby reducing the impact force at the moment of the robot's landing. The measured impact force at the robot's landing is 2086N, approximately 4.6 times the robot's weight, demonstrating that the design method proposed in this paper enables the robot to effectively handle significant impact forces, thereby enhancing its jumping capabilities. After several jumping tests, both the joints and structures of the designed robot have proven capable of successfully enduring such a substantial impact. Additional details can be found in [15].

In summary, the robot's fast response frequency, low inertia, high back-drivability, and high energy output capacity provide substantial evidence supporting the proposed methodology.

V. Conclusion

This article introduces a design and optimization approach for a bio-inspired humanoid robot capable of highly dynamic jumping. Design requirements were established based on studies of human jumping and theoretical calculations. The planetary joint and linear actuator were meticulously designed, with the linkage transmission and structure optimized to accommodate the characteristics of jumping motion. Simulations and experiments confirmed that the proposed method enables the robot to achieve a 0.5 m high jump and 1.1 m long jump,

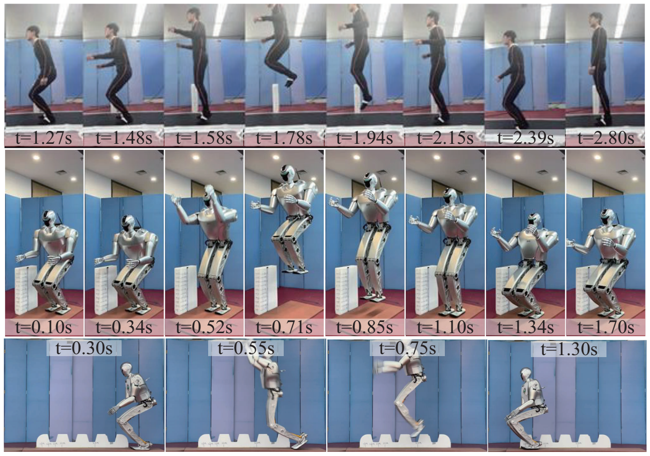

Fig. 3. Snapshots of human and robot high jumping and long jumping.

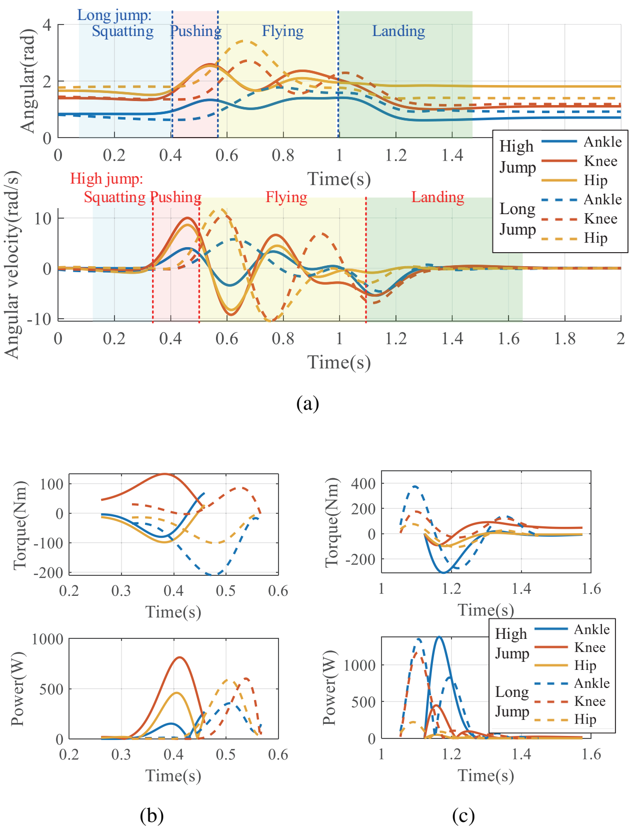

Fig. 4. Motion data of leg joints during robot jumping. (a) Leg joint angles and angular velocities. (b) Joint torques and powers at takeoff. (c) Joint torques and powers at landing.

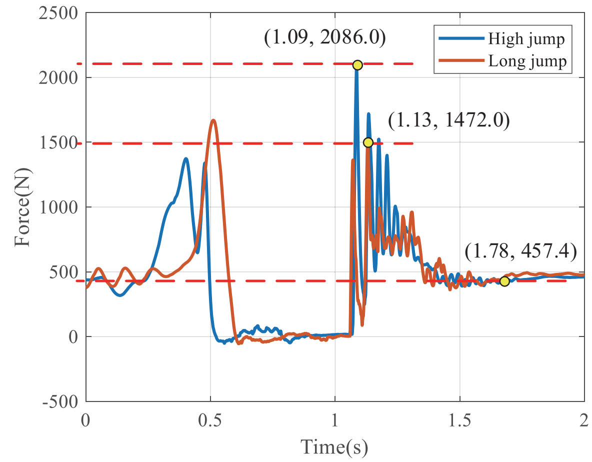

Fig. 5. Ground impact forces of robot during jumping motion.

indicating a high level of jumping ability for the robot. However, the current design is limited to three joints in the sagittal plane. In future work, additional joints will be considered to enable the robot to perform multimodal jumpings.

References

[1] J. Ramos and S. Kim, "Dynamic locomotion synchronization of bipedal robot and human operator via bilateral feedback teleoperation," *Science robotics*, vol. 4, no. 35, p. eaav4282.

[2] M. Sitti, A. Menciassi, A. J. Ijspeert, K. H. Low, and S. Kim, "Survey and introduction to the focused section on bio-inspired mechatronics," *IEEE/ASME Transactions on Mechatronics*, vol. 18, no. 2, pp. 409–418, 2013.

[3] Wang, Albert, Michael, Chuah, Meng, Yee, Hyun, Dong, Jin, and O. and, "Design principles for energy-efficient legged locomotion and implementation on the mit cheetah robot," *IEEE/ASME transactions on mechatronics*, vol. 20, no. 3, pp. 1117–1129, 2015.

[4] C. Dong, X. Chen, Z. Yu, H. Liu, F. Meng, and Q. Huang, "Swift running robot leg: Mechanism design and motion-guided optimization," *IEEE/ASME Transactions on Mechatronics*, 2023.

[5] L. Wang, L. Meng, R. Kang, B. Liu, S. Gu, Z. Zhang, F. Meng and A. Ming, " Design and Dynamic Locomotion Control of Quadruped Robot with Perception-Less Terrain Adaptation," *Cyborg and Bionic Systems*, vol. 4, 2023.

[6] K. Kojima, Y. Kojio, T. Ishikawa, F. Sugai, and M. Inaba, "Drive-train design in jaxon3-p and realization of jump motions: Impact mitigation and force control performance for dynamic motions," *IEEE*, 2020.

[7] Z. Li, X. B. Peng, P. Abbeel, S. Levine, G. Berseth, and K. Sreenath, "Robust and versatile bipedal jumping control through reinforcement learning," *Robotics: Science and Systems XIX, Daegu, Republic of Korea*, 2023.

[8] P. Xiang, L. Yan, Y. Guo, X. He, C. Gerada, and I.-M. Chen, "A concentrated-flux-type pm machine with irregular magnets and iron poles," *IEEE/ASME Transactions on Mechatronics*, 2023.

[9] F. Guenther, H. Q. Vu, and F. Iida, "Improving legged robot hopping by using coupling-based series elastic actuation," *IEEE/ASME Transactions on Mechatronics*, vol. 24, no. 2, pp. 413–423, 2019.

[10] W. Roozing, Z. Ren, and N. G. Tsagarakis, "An efficient leg with series–parallel and biarticular compliant actuation: design optimization, modeling, and control of the eleg," *The International Journal of Robotics Research*, vol. 40, no. 1, pp. 37–54, 2021.

[11] Q. Nguyen, M. J. Powell, B. Katz, J. Di Carlo, and S. Kim, "Optimized jumping on the mit cheetah 3 robot," in *2019 International Conference on Robotics and Automation (ICRA)*. IEEE, 2019, pp. 7448–7454.

[12] S. Lohmeier, T. Buschmann, and H. Ulbrich, "System design and control of anthropomorphic walking robot lola," *IEEE/ASME Transactions on Mechatronics*, vol. 14, no. 6, pp. 658–666, 2009.

[13] P. Seiwald, S.-C. Wu, F. Sygulla, T. F. Berninger, N.-S. Staufenberg, M. F. Sattler, N. Neuburger, D. Rixen, and F. Tombari, "Lola v1. 1–an upgrade in hardware and software design for dynamic multi-contact locomotion," in *2020 IEEE-RAS 20th International Conference on Humanoid Robots (Humanoids)*. IEEE, 2021, pp. 9–16.

[14] C. Zhang, W. Zou, L. Ma, and Z. Wang, "Biologically inspired jumping robots: A comprehensive review," *Robotics and Autonomous Systems*, vol. 124, p. 103362, 2020.

[15] H. Qi, X. Chen, Z. Yu, G. Huang, Y. Liu, L. Meng, and Q. Huang, "Vertical jump of a humanoid robot with cop-guided angular momentum control and impact absorption," *IEEE Transactions on Robotics*, 2023.